Journal of King Saud University - Science 36 (2024) 103186

HOSTED BY

Contents lists available at ScienceDirect

Journal of King Saud University - Science

journal homepage: www.sciencedirect.com

Full Length Article

Impact of fin material properties and the inclination angle on the thermal efficiency of evacuated tube solar water heater: An experimental study

Sorabh Aggarwal [a], Raj Kumar [a,b,*], Sushil Kumar [c], Tej Singh [d,*]

[a] Faculty of Engineering and Technology, Shoolini University, Solan, Himachal Pradesh 173229, India
[b] Department of Mechanical Engineering, Gachon University, Seongnam 13120, South Korea
[c] Department of Physics, Hansraj College, University of Delhi, Delhi 110007, India
[d] Savaria Institute of Technology, Faculty of Informatics, ELTE Eötvös Loránd University, Budapest 1117, Hungary

ARTICLE INFO

Keywords:
Evacuated tube solar collector
Heat pipe
Fin material
Solar water heater

ABSTRACT

In recent years, evacuated tube solar water heaters (ETSWH) have become popular due to their efficiency and low maintenance based on trends in India's solar thermal market. Numerous studies have focused on improving system performance. In the scientific literature, there is a lack of information on the selection of appropriate fin material and the benefits associated with it. The thermal efficiency (η_t) of ETSWH is directly impacted by the choice of fin material. In this context, the goal of this study was to assess the impact of copper and aluminum using fin material as well as the inclination angle on ETSWH's η_t. The experiments are conducted for mass flow rate (m_{wt}) varying from 2 to 5l/h. With a m_{wt} of 2l/h, the highest outlet temperature of 55°C was recorded, while the highest η_t was found at 41.2°C with a m_{wt} of 5l/h. At all m_{wt}, copper fin is more efficient than aluminum fin due to their superior thermal conductivity. Among the considered inclination angles, at an inclination angle of 30°, the efficiency of ETSWH is found to be optimal. ETSWH with a copper fin attains (η_t = 58.57%), which is more significant than the case when the aluminum fin is used (η_t = 51.50%).

Nomenclature

T_{out}	Outlet temperature, °C
T_{in}	Inlet temperature, °C
D_e	Inner diameter of evacuated tube,m
L_e	Length of evacuated tube,m
C_p	Specific Heat at constant pressure, J. $Kg^{-1}.°C^{-1}$
A	Evacuated tube's aperture area,m^2
Q_g	Collector useful power,W
Q_{in}	Incident solar power,W
I_s	Solar intensity,W/m^2
m_{wt}	Mass flow rate of water, l/h
N_d	Number of days of the year
CPC	Concentric parabolic concentrator
ETSC	Evacuated tube solar collector
PCM	Phase change material
PTSC	Parabolic trough solar collector

Greek symbols

η_t	Thermal efficiency
θ	Incline angle of the thermosyphon
α	Local latitude
δ	Declination angle
ω	Sun hour angle
τ	Transmittance of the atmosphere
ε	Earth's orbit correction factor

* Corresponding authors.
E-mail addresses: errajap@gmail.com (R. Kumar), sht@inf.elte.hu (T. Singh).

https://doi.org/10.1016/j.jksus.2024.103186
Received 27 October 2022; Received in revised form 2 March 2024; Accepted 28 March 2024
Available online 29 March 2024

1. Introduction

Solar energy is frequently used in industrial and residential water heating. Due to its simplicity, solar water heating is popular. Large-scale usage of petroleum derivatives, especially in the energy sector, has caused an energy crisis that has caused global warming, ozone layer depletion, and ecological disruptions (Jaoua and Hajji, 2020). The desire to cut greenhouse gas emissions and avert climate damage has made renewable energy important. Renewable energy sources for a pollution-free world need technology innovation (Ibrahim et al., 2020; Albdour et al., 2022; Nawsud et al., 2022). Nature replenishes renewable energy. Solar, hydro, marine, geothermal, wind, and other solar-fuelled energies are examples (Khan et al., 2022; AlArjani et al., 2021). As global energy demand rises, solar energy might be employed in almost every sector. Solar water heaters have been modified to enhance efficiency. Since efficiency has grown, residential and commercial solar thermal collector usage has expanded (Harrabi et al., 2021; Hazami et al., 2013). Solar collectors include concentrating, evacuated tube, and flat plate. Heat pipe evacuated solar tube collectors are gaining popularity due to their numerous benefits (Aggarwal et al., 2023; Reay et al., 2013; Aggarwal et al., 2021). Akyurt (1984) examined heat pipes as a heat transfer component in solar water heating systems. Heat pipes have been shown in a few studies to be effective heat absorbers for ETSCs (Murugan et al., 2022; Arif et al., 2022). A novel integrated collector storage solar water heater was tested using Standard ISO 9459-5's dynamic system testing technique, and the authors emphasized the usage of heat pipes as efficient heat absorbers in solar water heating systems (Messaouda et al., 2023; Elmosbahi et al., 2023). The effectiveness of solar water heaters has been improved using various strategies, including design modifications, flow rate optimization for optimal heat transfer, and alternative working fluids (Ghorab et al., 2017; Dhaou et al., 2022; Shafieian et al., 2019a; Shafieian et al., 2019b). Essa et al. (2021) compared innovative U-tube direct flow ETSC with three, seven, and eleven helical steps to standard ETSC. The new helical tube outperformed the traditional approach at 10, 20, and 30l/h. Seven-step innovative tubes had the greatest mean exergy and energy efficiencies of 18% and 38.6% at 30l/h. Bracamonte et al. (2015) performed experiments and Tri dimensional numerical simulations to determine how tilt angle affects flow patterns, energy conversion efficiency, and stratification. Bracamonte (2017) carried out simulations for four different transient energy inputs and 10°, 20°, 27° and 45° collector tilt angles. Dabra et al. (2013) using ETSC with collector tilt angles of 30° and 45° from horizontal. Experiments indicated that 30° ETSC had greater thermal performance than 45° ETSC. Jamil and Tiwari (2009) determined the optimal monthly and yearly tilt angles of collector and found that the optimal annual tilt angle was 30° in the autumn. Gholipour et al. (2020) carried out a study to enhance the efficiency of ETSC through the implementation of three distinct novel arrangements of absorbent tubes. The results suggested that helical coil ETSC exhibits a maximum efficiency of 55.1% while operating at m_{wt}=40l/h. Ayompe and Duffy (2013) assessed SWH thermal performance equipped with a heat pipe ETSC. The obtained findings showed that 70.3°C was the maximum water temperature that was reached at the exit. The results also indicated that the SWHs system's maximum efficiency was determined to be 52.0%. Xia and Chen (2020) examined mini-CPC-integrated ETSC collectors analytically and experimentally. They observed that CPC raised temperature 27.3%. The results showed that CPC had a 27.2% higher η_t than the traditional collector. Kiran et al. (2021) evaluated and compared the η_t of U-tube ETSC with parabolic reflectors and standard U-tube solar collectors. The study concluded that the η_t of the collector increases by 14.1% using a parabolic reflector.

Since heat pipe evacuated tube systems are expensive, they must be made more efficient to reduce their payback time. ETSWH system efficiency has been improved by researchers using different methods. Reflectors, nanofluids, optimal inclination angle, fin modification, and evacuated tube coating are used. Current research improves ETSWH performance with different fin materials and inclination angles. According to the literature research, fin and reflector material investigations are few. No research has compared fin materials' efficiency, to the author's knowledge. Novelty, the research simultaneously examined the impacts of fins materials and inclination angles on ETSWH efficiency. The study aims to examine:

1. the impact of fin materials on ETSWH heat gain and η_t.
2. the influence of the inclination angle on the T_{out} and ETSWH's η_t

2. Experimental parameters and construction

The different fin materials and inclination angles are used to enhance the performance of ETSWH. Copper and aluminium fins are employed at

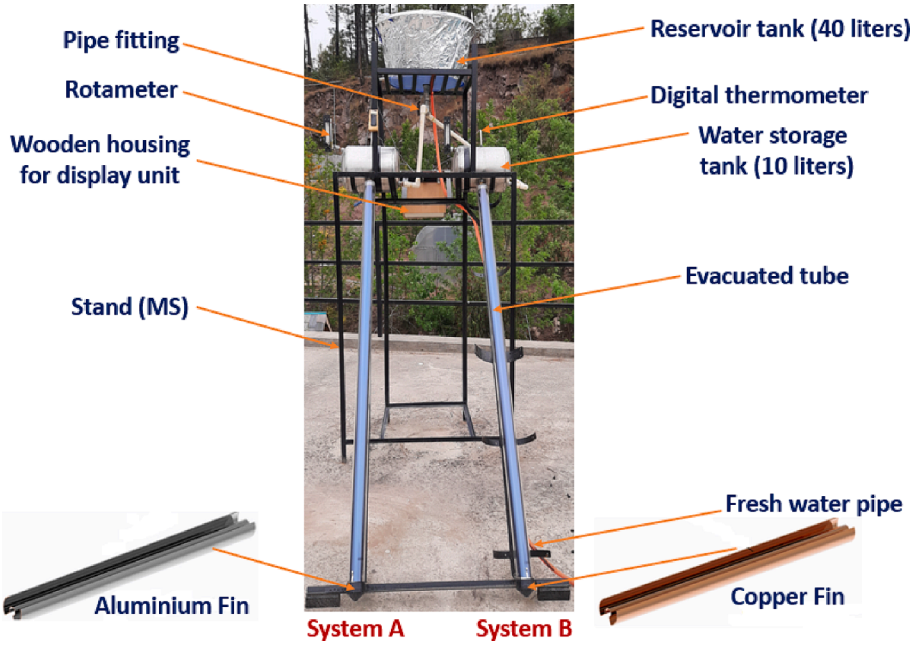

Fig. 1. Actual view of experimental set up.

20°, 30°, 40°, and 50° inclinations. Experiments are conducted for m_{wt} 2 to 5l/h. This study considers parameters from previous studies on ETSCs using water, which measured m_{wt} and tilt angle at 1-5l/h and 30° and 45°, respectively (Gholipour et al., 2020; Dabra et al., 2013).

Fig. 1 shows the experimental structure planned and built according to ASHRAE standards. The experimental setup has two identical evacuated tube collectors, A and B. System A uses an aluminum fin within the evacuated tube, whereas system B uses a copper fin. The 10-liter inner storage tanks are made of stainless steel, insulated with puff material, and covered. From their open end, tanks receive 1800mm evacuated tubes with 58mm outer diameters and 45mm inner diameters. The top has a 40-liter, completely insulated reservoir tank connected to the storage tanks via pipe connections. To fill the reservoir tank, a freshwater pipe is attached. The system is on a mild steel stand. Fig. 2a shows a rotameter at both storage tank outlets for flow monitoring and control. The rotameter ranges from 2 to 20l/h with ±3% of accuracy. The digital thermometer has a range of (−50 to 200) °C, with an accuracy of ±1 °C monitors hot and cold-water temperature. A real image of a digital thermometer is shown in (Fig. 2b). Fig. 2c shows wooden casing for display units.

3. Experimental procedure

To perform experiments, a continuous supply of fresh water is needed, and this is provided by the reservoir tank seen in (Fig. 1). Both collectors' water storage tanks get cold water from the tank intake line at the bottom. The bottom tank intake line supplies cold water to collectors' water storage tanks. As illustrated in Fig. 2b, digital thermometer measures storage tank water temperature. As the sun shines, evacuated tubes absorb the majority of the heat. This absorbed heat is transferred to the heat pipe positioned in the evacuated tube via the fins surrounding the heat pipe. Transported heat raises the evaporator section's temperature, heating the heat pipe refrigerant. The refrigerant goes into the condenser and heats the water surrounding it as it turns liquid to gas. Refrigerant liquidifies and goes to the evaporator for the next cycle. The thermosyphon mechanism causes the heated water in the tank to rise to the top of the tank surface. Evaporator and condenser sections of the heat pipe remained in the tube and tank, respectively.

The experiment was carried out at Shoolini University in Solan, India, in March and April. Every hour from 9:00 a.m. to 4:00 p.m., observations are taken. The rotameter was set to a specific value: a certain flow rate (2 to 5l/h), and readings were taken every hour. The experiment uses two heat pipe evacuated tube systems with varying m_{wt}. One heat pipe evacuated tube system contains copper fin and the other aluminum. Both single-tube systems include 10-liter storage tanks. Puff insulation was used to maximize heat retention in tanks. The heat pipe evacuated tube systems are set at 20°, 30°, 40°, and 50° inclinations to maximize sun radiation. A rotameter measured m_{wt}. Pyranometer record sun intensity with an accuracy of ±5% and range from 0 to 1800 W/m^2. Digital thermometers measured water temperature.

3.1. Performance analysis

The heat transfer from evacuated tube to water is computed as heat gain (Q_g) per unit time (output power):

$$Q_g = m_{wt} C_p (T_{out} - T_{in}) \tag{1}$$

If I_s is the input power that is received by the evacuated tubes. The input power is given as (Jasim et al., 2020):

$$Q_{in} = qA \tag{2}$$

$$q = I_s \varepsilon \tau [sin\delta \sin(\theta - \alpha) + cos\delta \cos(\theta - \alpha) cos\omega] \tag{3}$$

The earth's orbit correction factor, denoted by ε, may be calculated using the following equation (Jasim et al., 2021; Handbook, 1985):

$$\varepsilon = (1 + 0.033 \cos(360 N_d / 365)] \tag{4}$$

However, in the current experimentation Q_{in} is computed as given below:

$$Q_{in} = I_s A \tag{5}$$

I_s is taken directly from the pyranometer.

The η_t of ETSWH is computed using following formula:

$$\eta_t = \frac{Q_g}{Q_{in}} \tag{6}$$

According to (Veena et al., 2021; Ma et al., 2010) equation (7) may calculate the aperture area of evacuated tube, A.

$$A = 2 D_e L_e \tag{7}$$

4. Uncertainty analysis

The uncertainties in the measuring instruments (Kline and McClintock, 1953; Wang et al., 2017; Harrabi et al., 2020) employed in the current experiment is given in section 2 and 3. The maximum uncertainty in the η_t was determined to be 5.9% as illustrated in the supplementary file.

5. Results and analysis

Depending on the weather, the experiments are carried out on particular days. Experiments are carried out from 9:00 hours to 16:00 hours on clear sky days. The measurements are made on evacuated tubes with fins made of copper and aluminium at various m_{wt}. For maximum performance, the inclination angles are also optimized (Jamil and Tiwari, 2009).

5.1. ETSWH with copper as fin material

While experimenting, the variations in I_s over a 1-hour period are

Fig. 2. (a) Rotameters (b) Digital thermometer (c) Display units.

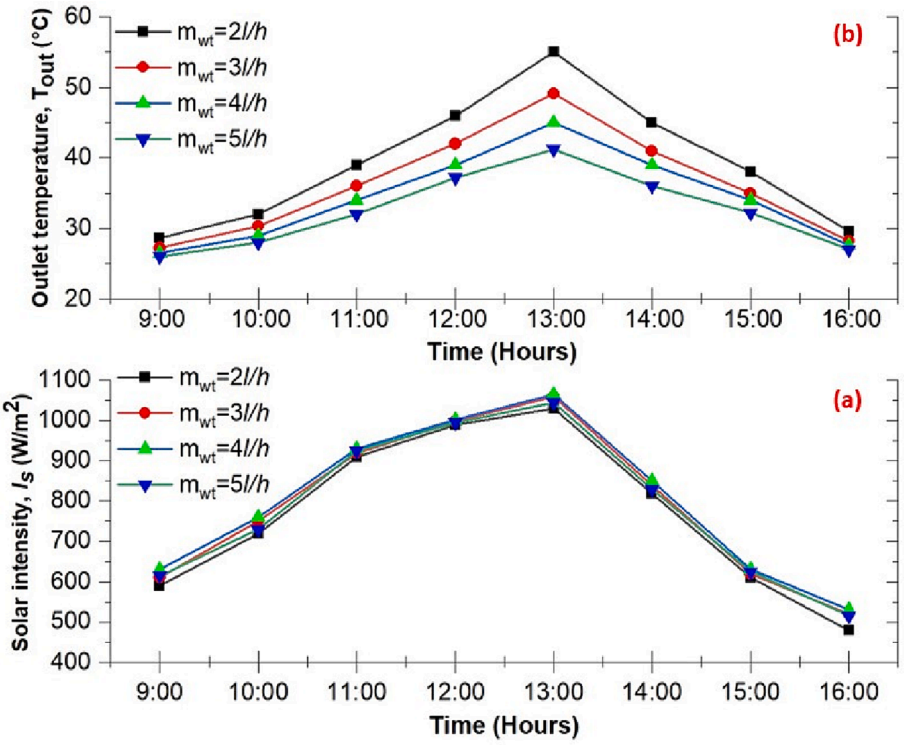

Fig. 3. Solar intensity (a) and T_{out} (b) variation for ETSWH with copper fin.

measured. On the site, I_s ranges from 590 W/m^2 to 1065 W/m^2. Numerous severe solar over irradiance occurrences, with observed values over 1367 W/m^2 up to 1845 W/m^2, lasting from seconds to minutes have also been studied (Do Nascimento et al., 2019). The site gets 785 W/m^2 average sun irradiation during testing. As seen in Fig. 3a, the sun irradiation reaches its peak (1065 W/m^2) at 13:00 hours and is. Such high solar irradiance of 1065 W/m^2 has been observed for very short moments during experimental runs. Over the trial days, the water's input temperature ranges from 19 to 25°C, averaging 23°C. In the first experimental run, ETSWH is provided a copper fin material and mounted at 30° since some study publications concluded that 30° tilt angle is ideal for ETSWH best performance (Dabra et al., 2013; Jamil

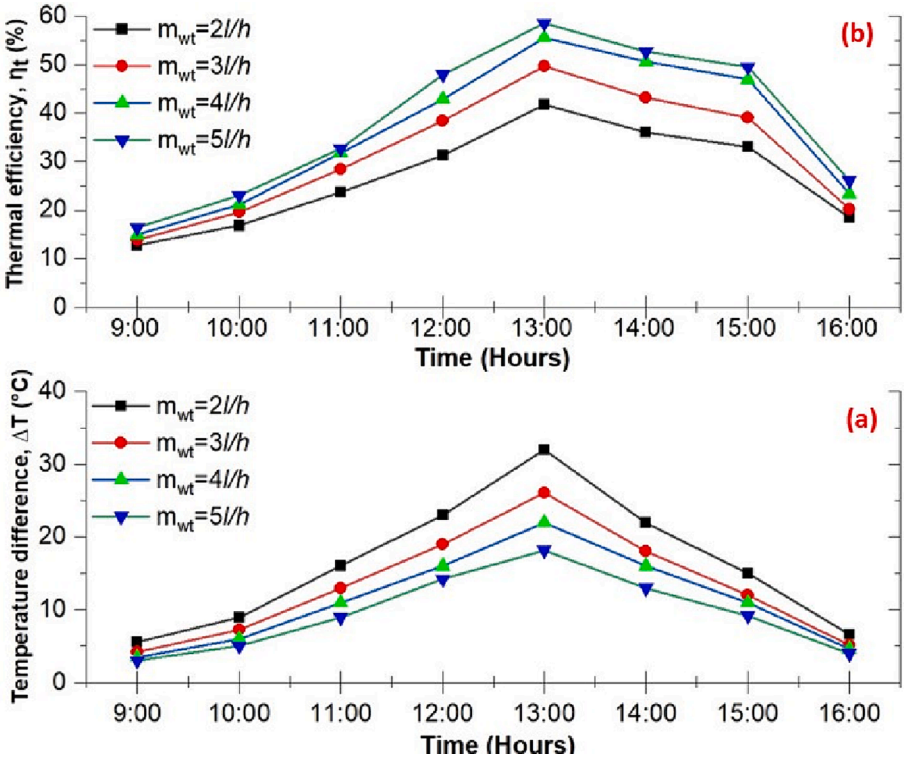

Fig. 4. Variation of ΔT (a) and η_t(b) of ETSWH with copper fin.

and Tiwari, 2009). The temperature of the outlet (T_{out}) is listed at different m_{wt}. The variation of T_{out} at different m_{wt} is depicted in Fig. 3b. The current study assumed m_{wt} ranged from 2 to 5l/h for a 10-litre storage tank, based on the study (Gholipour et al., 2020). The maximum T_{out} is observed at the optimum value of I_s during the day for all m_{wt} values. The highest T_{out} of 55°C is observed for the lowest m_{wt} of 2l/h, and the lowest T_{out} 26°C is observed at the highest m_{wt} of 5l/h. Fig. 3b shows that T_{out} of water decreases with a rise in m_{wt} value. This decrease is because of low residence time inside the ETSWH due to high velocity at enhanced m_{wt}. At lower m_{wt}, the T_{out} increases considerably at the expense of the amount of absorbed energy. The highest T_{out} achieved are 55, 49.1, 45, and 41.2°C at m_{wt} of 2, 3, 4, and 5l/h, respectively. Optimising the m_{wt} in direct response to solar radiation significantly improves the performance of the system.

Efficient ETSWH system design relies on the inlet-outlet temperature differential (ΔT). Fig. 4a shows the computed ΔT values, which followed the same pattern as T_{out} throughout the day. The heat-carrying capacity of fluid changes with m_{wt}, Despite ETSWH heat energy is almost constant. In Fig. 4a, ΔT decreases when water m_{wt} increases due to greater fluid speed, resulting in shorter heat transfer contact duration. At m_{wt} of 5l/h, the lowest ΔT was 18.2°C, whereas at 2l/h, it rose about 55% to 32°C. Fig. 4b, depicts ETSWH η_t at various m_{wt}. The ETSWH η_t rises as m_{wt} rises. The increase in m_{wt} enhances water heat-carrying capacity and heat gain. Increased heat gains enhance ETSWH η_t. The optimum values of η_t of the ETSWH achieved at 2, 3, 4, and 5l/h are 41.8, 49.5, 55.59, and 58.57%, respectively. The highest η_t (58.57%) of the ETSWH is recorded for m_{wt} of 5l/h and remains nearly 40% higher than the lowest recorded η_t (41.80%) for 2l/h, respectively.

5.2. ETSWH with aluminium as fin material

In the second experiment, ETSWH has aluminum fin and is positioned at 30° inclination angle. As the day progresses on, the I_s (Fig. 5a) increases, and the T_{out} exhibits the same pattern. At 13:00 hours, the sun's radiation intensity reaches its maximum value of 1050 W/m^2. At various m_{wt}, the T_{out} is measured. Fig. 5b, depicts the fluctuation in T_{out} for different m_{wt}. For every m_{wt}, the maximum T_{out} is seen at maximum I_s. The lowest T_{out}, 26°C, is seen for the highest m_{wt} (i.e., 5l/h), whereas the highest T_{out}, 51°C, is observed for the lowest m_{wt} of 2l/h. The T_{out} of the water decreases as m_{wt} of water increases. This decrease is due to low residence time within the ETSWH due to high velocity at enhanced m_{wt}. The maximum T_{out} values were attained for temperatures of 51°C, 46.2°C, 41.9°C, and 39°C, respectively, for m_{wt} of 2, 3, 4, and 5l/h, respectively.

Fig. 6a shows ΔT variation for aluminum fin at various m_{wt}. It follows the same pattern of I_s, rising during the day and falling after 13:00. Because more water needs to be heated for almost the same I_s, the ΔT for low m_{wt} is larger than that for high flow rates. The maximum ΔT of 28°C is recorded for the lowest m_{wt} (i.e. 2l/h). With increase in m_{wt}, the ΔT found to decrease and remains lowest (16°C) for the highest m_{wt} (i.e. 5l/h). The decrease in ΔT for the high m_{wt} (i.e. 5l/h) in comparison to low m_{wt} (i.e. 2l/h) is almost 43%. The η_t of an ETSWH with aluminium fins at various m_{wt} is shown in (Fig. 6b). The ETSWH η_t is further enhanced by the increase in m_{wt}, which also enhances heat gain. The ETSWH η_t reaches 36.93%, 44.59%, 48.90%, and 51.50% at 2, 3, 4, and 5l/h, respectively. The highest η_t (51.50%) of the ETSWH is recorded for m_{wt} of 5l/h and remains nearly 40% higher than the lowest recorded η_t (36.93%) for 2l/h, respectively.

5.3. Comparison of ETSWH with copper and aluminium as fin material

With copper and aluminium serving as the fin materials, the η_t of ETSWH at various m_{wt} is determined and displayed in (Figs. 4b and 6b), respectively. The largest m_{wt} of 5l/h results in the most incredible η_t. Fig. 7, compares the ΔT and η_t of ETSWH for copper and aluminium fin materials at a high m_{wt} of 5l/h. Aluminum fin have lower thermal conductivity than copper fin, resulting in lower ΔT. Copper has a larger morning-to-evening temperature differential (>18%) than aluminum, however during peak noontime, difference is 13%. Copper loses more heat than aluminum at high temperatures due to its superior thermal conductivity. The maximum temperature and thermal efficiency obtained using two fin materials have the same trend.

The η_t of ETSWH with copper fin rises from 16.41 to 58.57% with the passage of daytime, while decreasing after peaking at 13:00 hours.

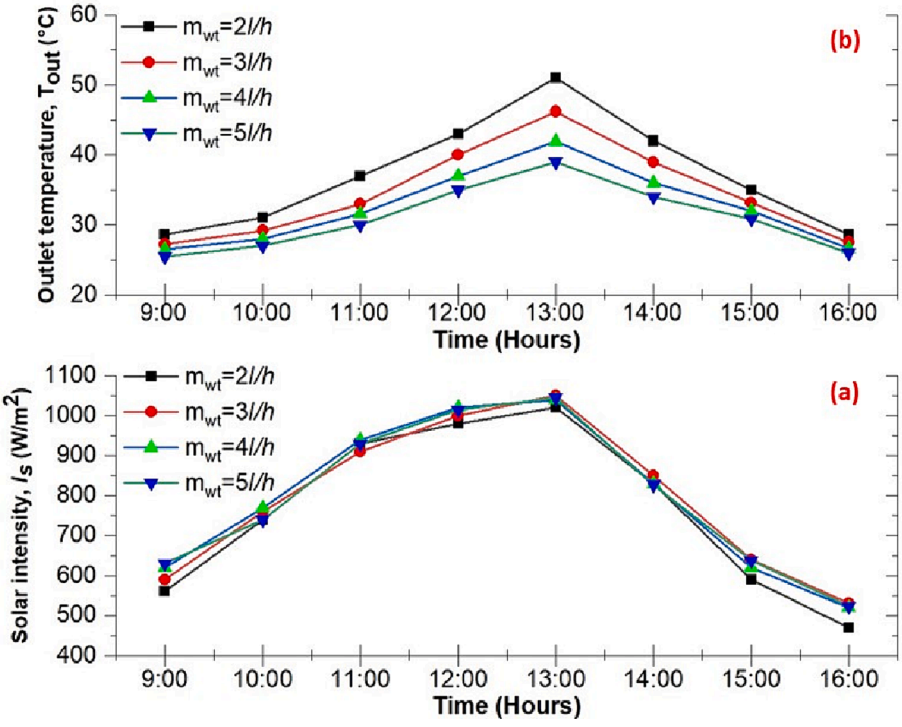

Fig. 5. Variation of I_s (a) and T_{out} (b) of ETSWH with aluminium fin.

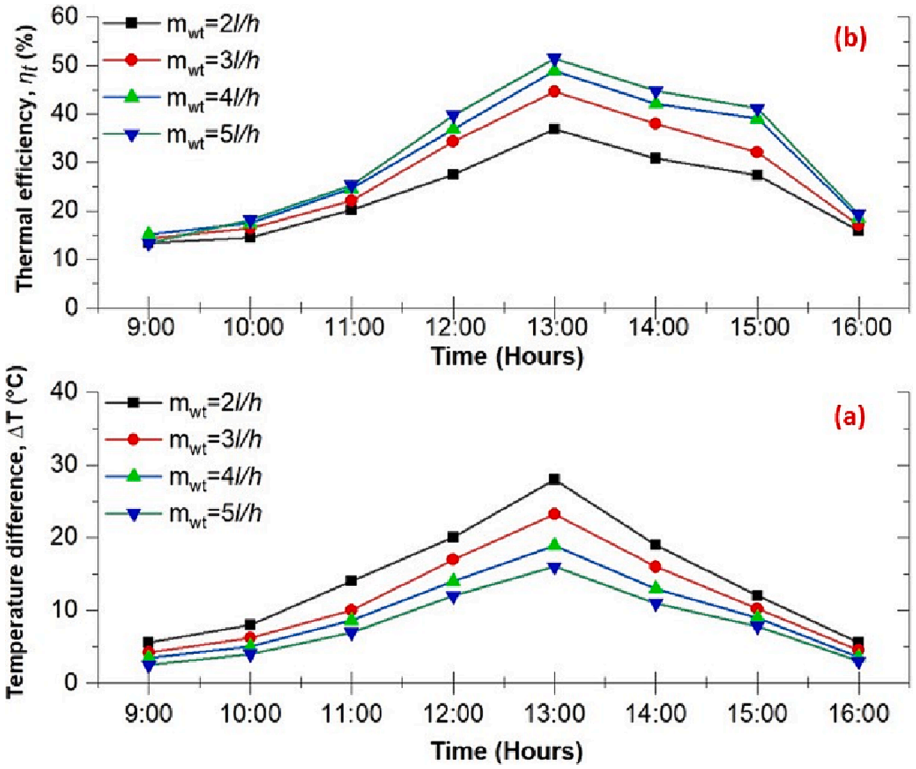

Fig. 6. Variation of ΔT (a) and η_t (b) of ETSWH with aluminium fin.

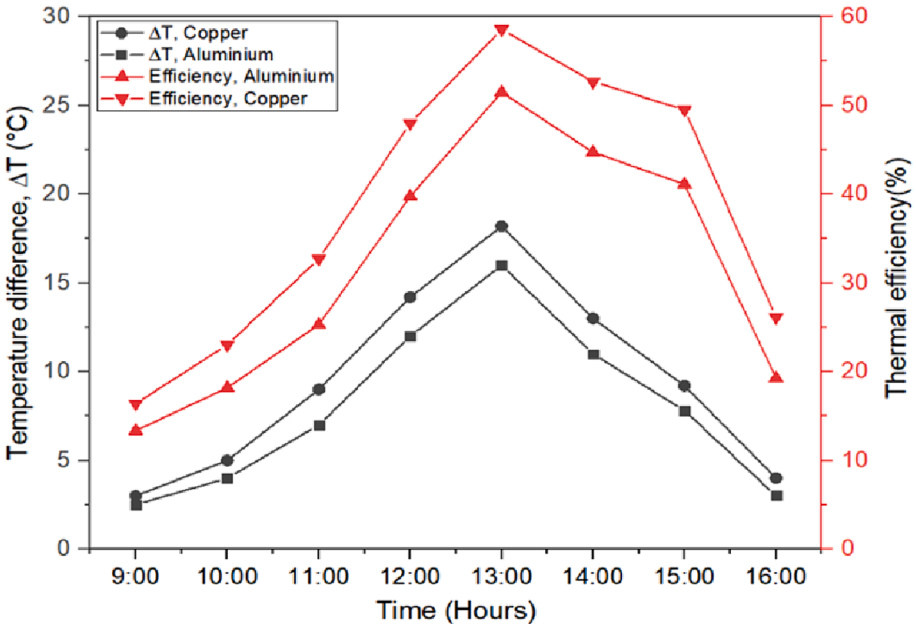

Fig. 7. Comparison of ΔT and η_t of ETSWH with copper and aluminium as fin material.

ETSWH with aluminium fins follows the similar pattern of η_t, increasing from 13.35% to 51.50% for morning hour to peak at noon and starts to decrease after attaining the peak at 13:00 hours. This tendency is understandable since the ETSWH η_t is related to the difference in intake and T_{out}. The η_t of the ETSWH for copper and aluminium is obtained at m_{wt} of 5*l*/*h*, and the maximum η_t is 58.57 and 51.50%, respectively. The temperature difference is dominant at noon, resulting in the highest η_t. Fig. 7 further shows that the maximum η_t of ETSWH with copper and aluminum fins varied by more than 20% throughout the evening and morning hours. In comparison, the difference is about 14% at the noon hour. This trend suggests that copper-finned ETSWH extracts more heat than aluminum-finned ones.

5.4. Impact of inclination angle on the efficiency of ETSWH having copper fin

Latitude, tilt angle, surface azimuth angle, and time of day may be changed to maximize solar radiation. The collector's inclination angle

may be adjusted to enhance radiation flow. According to Duffie and Beckman's "rules of thumb" (Duffie and Beckman, 2013) the ideal surface faces the equator and slopes equivalent to latitude for maximum yearly energy availability. The experimental setup is placed at Shoolini University's latitude and longitude, which are 30.86° N and 77.11° E, respectively. The collector is stationary and oriented southward to optimise solar energy absorption throughout the year. Fig. 8a, shows the variation in I_s and T_{out} of ETSWH with copper fin at different inclination angles and at m_{wt} of 5l/h. With time, the I_s increases for all inclination angles, and it starts to fall after attaining a peak at 13:00 hour. The highest solar radiation of 1065 W/m^2 was recorded for an inclination angle of 30° at 13:00 hours. The T_{out} (Fig. 8b) also follows the same pattern as solar radiations, i.e., it increases from 20° to 30° inclination angle and decreases afterward. Also, the T_{out} increases with time, and after attaining maximum values at 13:00 hours started to fall. The ultimate T_{out} of 41.2°C was recorded for an inclination angle of 30° at 13:00 hours, which is almost 18% higher than the T_{out} recorded at 50° at 13:00 hours.

Figs. 9(a and b) shows the variation in ΔT and η_t of ETSWH with copper fin at different inclination angles and at m_{wt} of 5l/h, respectively. As presented in (Fig. 9a) the ΔT increases with daytime and remains highest (18.2°C) for an inclination angle of 30° at 13:00 hours, whereas it remains 12°Cat inclination angle of 50° for the peak hour i.e. 13:00 hours. The trend for the η_t (Fig. 9b) of the ETSWH with copper at different inclination angles is the same as the maximum temperature attained by ETSWH. The η_t of the ETSWH starts increasing with the daytime passage and, after reaching the highest values at 13:00 hours, starts decreasing. Given that the η_t of solar water heaters is directly related to the temperature difference, this efficiency trend is acceptable. The temperature difference is dominant at noon hours. Fig. 9b also depicts that during peak hour, the lowest η_t (39.19%) was recorded at an inclination angle of 50°; it increases by almost 45% and remains highest (58.57%) at an inclination angle of 30°.

6. Comparison to previous studies

The present system's efficiency is compared to the previous analysis, as seen in Table S1 (supplementary information). In terms of maximum η_t, helical coil ETSC achieved 55.1% at a m_{wt}=40l/h (Gholipour et al., 2020) and heat pipe ETSC attained 52% (Ayompe and Duffy, 2013). ETSC tilted at 30°, had superior η_t compared to the ETSC tilted at 45° (Dabra et al., 2013). ETSC with CPC reflector, η_t enhanced by 27.2% (Xia and Chen, 2020) and U-tube ETSC with parabolic reflector, η_t increased by 14.1% compared to conventional ETSC (Kiran et al., 2021). In the present research, ETSWH is integrated with two different types of fins materials as well as the inclination angle and its effect on the η_t is investigated. The experimental findings shows that ETSWH integrated copper fin achieves the highest η_t of 58.57% and when the tilt angle of ETSWH is set to 30° and m_{wt}= 5l/h. The ETSWH integrated copper fin achieves the highest T_{out} of 55°C at m_{wt}= 2l/h. Table S1 clearly demonstrates a substantial improvement in η_t in the current research compared to previous work.

7. Conclusions

The thermal performance of ETSWH has been examined experimentally using copper and aluminium fins at distinct collector inclination angles and mass flow rates. Experiments show that the fin material and collector inclination angle have a considerable impact on ETSWH thermal performance. The following findings are drawn from the investigations:

1. Reducing the m_{wt}, increases the T_{out} of the ETSWH but decreases the absorbed heat gain and η_t. The highest T_{out} is obtained for ETSWH at a low m_{wt} (2l/h) at an inclination angle of 30°. The largest heat gain obtained for ETSWH at m_{wt} of 5l/h at an inclination angle of 30°.
2. The higher T_{out} is obtained for ETSWH having copper as a fin material compared to that with aluminium. It was found that copper fins outperform aluminium fins because of their higher thermal conductivity.

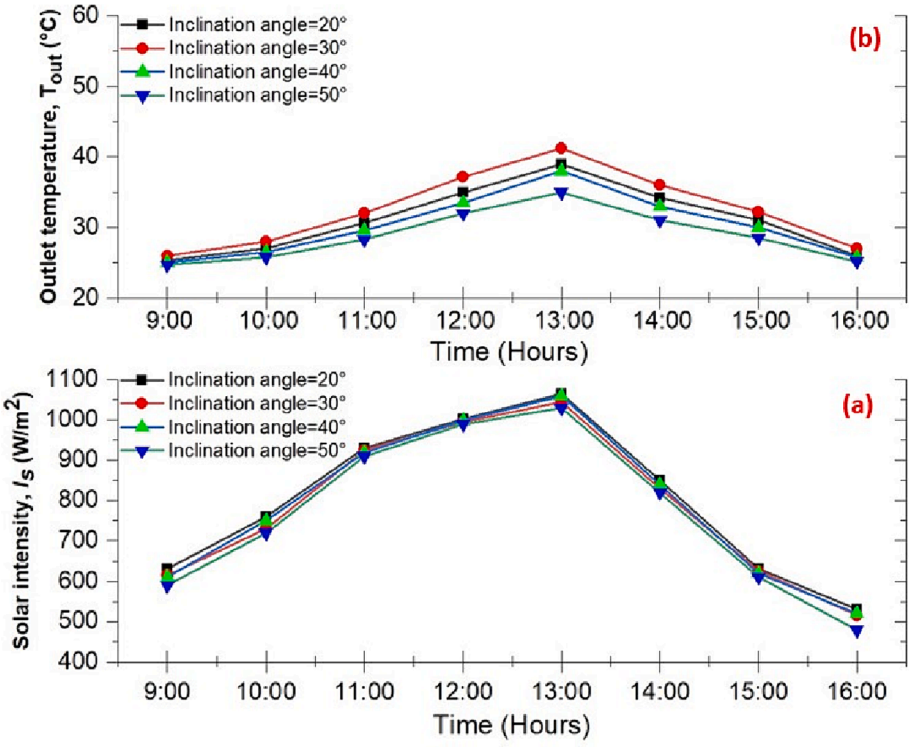

Fig. 8. Variation of I_s (a) and T_{out}(b) of ETSWH with copper fin at different inclination angles and at m_{wt} of 5l/h.

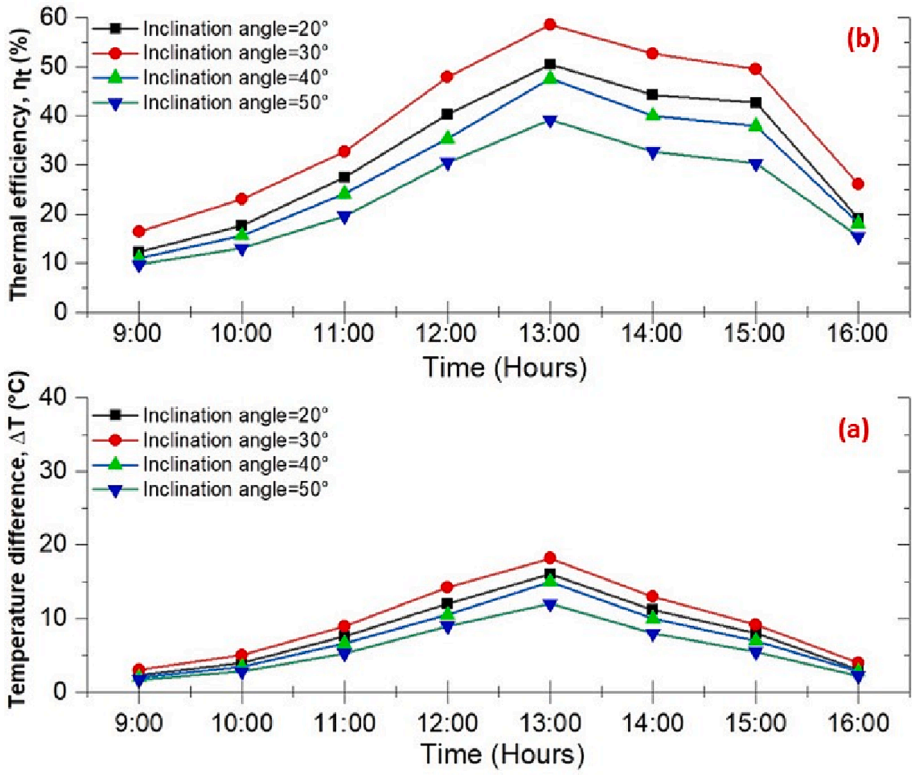

Fig. 9. Variation of ΔT (a) and η_t (b) of ETSWH with copper at different inclination angles and at m_{wt} of 5l/h.

3. The ETSWH with inclination angle of 30°, the performance is relatively superior compared to other inclination angles. The highest η_t of ETSWH with copper fins and m_{wt} of 5l/h occurs at 30° inclination angle.

The future scope for research in this area seems promising, as there are several avenues for further investigation and development. One area for future research could be to examine the consequences of reflectors and energy storage systems on the η_t of ETSWH. Another area for future research could be the use of multicriteria decision-making techniques to optimize the parameters that influence the η_t of the ETSWH.

CRediT authorship contribution statement

Sorabh Aggarwal: Conceptualization, Data curation, Visualization, Investigation, Formal analysis, Methodology, Writing – original draft, Writing – review & editing. **Raj Kumar:** Conceptualization, Visualization, Investigation, Validation, Formal analysis, Methodology, Supervision, Resources, Writing – review & editing. **Sushil Kumar:** Conceptualization, Data curation, Formal analysis, Visualization, Methodology, Writing – review & editing. **Tej Singh:** Conceptualization, Formal analysis, Investigation, Methodology, Validation, Visualization, Writing – review & editing.

Appendix A. Supplementary material

Supplementary data to this article can be found online at https://doi.org/10.1016/j.jksus.2024.103186.

References

Aggarwal, S., Kumar, S., Kumar, R., Robin Thakur, R., 2021. Thermal augmentation in evacuated tube solar collectors using reflectors, nano fluids, phase change materials and tilt angle: a review. Mater. Today:. Proc. 45, 4931–4935.

Aggarwal, S., Kumar, R., Lee, D., Kumar, S., Singh, T., 2023. A comprehensive review of techniques for increasing the efficiency of evacuated tube solar collectors. Heliyon. 9, e16390.

Akyurt, M., 1984. Development of heat pipes for solar water heaters. Sol. Energy 32 (5), 625–631.

AlArjani, A., Modibbo, U.M., Ali, I., Sarkar, B., 2021. A new framework for the sustainable development goals of Saudi Arabia. J. King Saud Univ.-Sci. 33 (6), 101477.

Albdour, S.A., Haddad, Z., Sharaf, O.Z., Alazzam, A., Abu-Nada, E., 2022. Micro/nano-encapsulated phase-change materials (ePCMs) for solar photothermal absorption and storage: fundamentals, recent advances, and future directions. Prog. Energy Combust. Sci. 93, 101037.

Arif, M.N., Waqas, A., Butt, F.A., Mahmood, M., Khoja, A.H., Ali, M., Ullah, K., Mujtaba, M.A., Kalam, M.A., 2022. Techno-economic assessment of solar water heating systems for sustainable tourism in northern Pakistan. Alex. Eng. J. 61 (7), 5485–5499.

Ayompe, L.M., Duffy, A., 2013. Thermal performance analysis of a solar water heating system with heat pipe evacuated tube collector using data from a field trial. Sol. Energy 90, 17–28.

Bracamonte, J., 2017. Effect of the transient energy input on thermodynamic performance of passive water-in-glass evacuated tube solar water heaters. Renew. Energy 105, 689–701.

Bracamonte, J., Parada, J., Dimas, J., Baritto, M., 2015. Effect of the collector tilt angle on thermal efficiency and stratification of passive water in glass evacuated tube solar water heater. Appl. Energy 155, 648–659.

Dabra, V., Yadav, L., Yadav, A., 2013. The effect of tilt angle on the performance of evacuated tube solar air collector: experimental analysis. Int. J. Eng. Sci. Technol. 5 (4), 100–110.

Dhaou, M.H., Mellouli, S., Alresheedi, F., El-Ghoul, Y., 2022. Experimental assessment of a solar water tank integrated with nano-enhanced PCM and a stirrer. Alex. Eng. J. 61 (10), 8113–8122.

Do Nascimento, L.R., de Souza Viana, T., Campos, R.A., Rüther, R., 2019. Extreme solar overirradiance events: Occurrence and impacts on utility-scale photovoltaic power plants in Brazil. Sol. Energy 186, 370–381.

Duffie, J.A., Beckman, W.A., 2013. Solar engineering of thermal processes. John Wiley & Sons.

Elmosbahi, M.S., Hamdi, M., Hazami, M., 2023. Design and experimental analysis of heat transfer performance of a two-phase closed thermosyphon system. J. Appl. Mech. Tech. Phys. 64 (5), 144–158.

Essa, M.A., Asal, M., Saleh, M.A., Shaltout, R.E., 2021. A comparative study of the performance of a novel helical direct flow U-Tube evacuated tube collector. Renew. Energy 163, 2068–2080.

Gholipour, S., Afrand, M., Kalbasi, R., 2020. Improving the efficiency of vacuum tube collectors using new absorbent tubes arrangement: introducing helical coil and spiral tube adsorbent tubes. Renew. Energy 151, 772–781.

Ghorab, M., Entchev, E., Yang, L., 2017. Inclusive analysis and performance evaluation of solar domestic hot water system (a case study). Alex. Eng. J. 56 (2), 201–212.
Handbook, A., 1985. Fundamentals. American Society of Heating, Refrigerating, and Air Conditioning Engineers, Inc., Atlanta, Georgia.
Harrabi, I., Hamdi, M., Hazami, M., 2020. Assessment of uncertainties in energetic and exergetic performances of a flat plate solar water heater. Math. Probl. Eng. 2020, 6671576.
Harrabi, I., Hamdi, M., Bessifi, A., Hazami, M., 2021. Dynamic modeling of solar thermal collectors for domestic hot water production using TRNSYS. Euro-Mediterranean J. Environ. Integrat. 6, 1–17.
Hazami, M., Kooli, S., Naili, N., Farhat, A., 2013. Long-term performances prediction of an evacuated tube solar water heating system used for single-family households under typical Nord-African climate (Tunisia). Sol. Energy 94, 283–298.
Ibrahim, I.D., Sadiku, E.R., Jamiru, T., Hamam, Y., Alayli, Y., Eze, A.A., 2020. Prospects of nanostructured composite materials for energy harvesting and storage. J. King Saud Univ.-Sci. 32 (1), 758–764.
Jamil, A.M., Tiwari, G.N., 2009. Optimization of tilt angle for solar collector to receive maximum radiation. The Open Renew. Energy J. 2, 19–24.
Jaoua, N., Hajji, W., 2020. Gaussian models for anthropogenic CO2 emissions consistent with prescribed climate targets. J. King Saud Univ.-Sci. 32 (7), 3119–3124.
Jasim, A.K., Freegah, B., Alhamdo, M.H., 2020. Numerical and experimental study of a thermosyphon closed-loop system for domestic applications. Heat Transfer. 1–21.
Jasim, A.K., Abbood, B.H., Alhamdo, M.H., 2021. Investigative study of thermal performance of thermosyphon solar collector. J. Eng. Sustain. Dev. 25 (2), 46–57.
Khan, Z.A., Hussain, T., Baik, S.W., 2022. Boosting energy harvesting via deep learning-based renewable power generation prediction. J. King Saud Univ.-Sci. 34 (3), 101815.
Kiran, N.B., Premnath, S., Muthukumar, P., 2021. Performance comparison of evacuated U-tube solar collector integrated parabolic reflector with conventional evacuated U-tube solar collector. Sādhanā 46, 1–11.
Kline, S.A., McClintock, F.A., 1953. Describing uncertainties in single-sample experiments. Mech. Eng. 1953, 3–8.
Ma, L., Lu, Z., Zhang, J., Liang, R., 2010. Thermal performance analysis of the glass evacuated tube solar collector with U-tube. Build. Environ. 45, 1959–1967.
Messaouda, A., Hamdi, M., Hazami, M., Guizani, A.A., 2023. Dynamic testing of a new integrated collector storage solar water heater (ICSSWH) according to standard ISO 9459–5: Use of a numerical approach for long-term prediction in different climatic conditions. Environ. Prog. Sustain. Energy 14254.
Murugan, M., Saravanan, A., Elumalai, P.V., Kumar, P., Saleel, C.A., Samuel, O.D., Setiyo, M., Enweremadu, C.C., Afzal, A., 2022. An overview on energy and exergy analysis of solar thermal collectors with passive performance enhancers. Alex. Eng. J. 61 (10), 8123–8147.
Nawsud, Z.A., Altouni, A., Akhijahani, H.S., Kargarsharifabad, H., 2022. A comprehensive review on the use of nano-fluids and nano-PCM in parabolic trough solar collectors (PTC). Sustain. Energy Technol. Assess. 51, 101889.
Reay, D., McGlen, R., Kew, P., 2013. Heat pipes: theory, design and applications. Butterworth-Heinemann.
Shafieian, A., Khiadani, M., Nosrati, A., 2019a. Thermal performance of an evacuated tube heat pipe solar water heating system in cold season. Appl. Therm. Eng. 149, 644–657.
Shafieian, A., Osman, J.J., Khiadani, M., Nosrati, A., 2019b. Enhancing heat pipe solar water heating systems performance using a novel variable mass flow rate technique and different solar working fluids. Sol. Energy 186, 191–203.
Veena, K.A., Arjunan, T.V., Seenivasan, D., Venkatramanan, R., Vijayan, S., 2021. Techno-Economic evaluation of an evacuated tube solar air collector with inserted baffles. Proc. Inst. Mech. Eng. Part E: J. Process Mech. Eng. 235 (4), 1027–1038.
Wang, Z.Y., Diao, Y.H., Liang, L., Zhao, Y.H., Zhu, T.T., Bai, F.W., 2017. Experimental study on an integrated collector storage solar air heater based on flat micro-heat pipe arrays. Energ. Build. 152, 615–628.
Xia, E.T., Chen, F., 2020. Analyzing thermal properties of solar evacuated tube arrays coupled with mini-compound parabolic concentrator. Renew. Energy 153, 155–167.